Environ Monit Assess (2008) 145:135–143
DOI 10.1007/s10661-007-0023-6

The role of atmospheric circulation system playing in coupling relationship between spring NPP and precipitation in East Asia area

Yu Deyong · Zhu Wenquan · Pan Yaozhong

Received: 8 February 2007 / Accepted: 30 October 2007 / Published online: 30 November 2007
© Springer Science + Business Media B.V. 2007

Abstract In many East Asia regions, spring (from March to May) precipitation is an important restricting factor to vegetation growth, and atmospheric circulation system may influence spring precipitation patter. It is helpful to under the response of ecosystem to climate change by studying the influence of atmospheric circulation system on the coupling relationship between spring net primary productivity and precipitation. Driving CASA (Carnegie-Ames-Stanford Approach) NPP (Net Primary Productivity) model, we estimated spring NPP for East Asia area (70°E–1 70°E, 10°N–70°N) from 1982 to 1999, and by the method of singular value decomposition we further analyzed the coupling features of spring NPP with precipitation. The result showed that the response features of NPP to precipitation were mainly embodied within the leading six NPP-precipitation paired-modes. The interpretation rates of the leading six paired-modes to the covariance of NPP-precipitation were 42.91, 23.29, 9.96, 5.60, 5.04 and 3.95%, respectively, and total to 90.75%. The temporal correlation coefficients of the leading six paired-modes were 0.830, 0.889, 0.841, 0.747, 0.912 and 0.923, respectively, and all the correlations were significant at significant level of 0.001. In some high latitude regions, there was no obviously corresponding relationship between NPP and precipitation in the leading two paired-modes, and the reason of it may be that spring temperature was the main restricting factor to NPP. In middle and low latitude regions, the effect of precipitation on NPP was relatively more notable. Nine atmospheric circulation factors in spring affected the patterns of NPP and precipitation greatly, and the regions with interpretation rate over 50% shared 60.41 and 65.58% of the whole study area, respectively.

Keywords Net primary productivity · Precipitation · Coupling feature · Atmospheric circulation factor · Remote sensing

Y. Deyong
State Key Laboratory of Urban and Regional Ecology,
Research Center for Eco-Environmental Sciences,
Chinese Academy of Science,
Beijing 100085, People's Republic of China

Y. Deyong · Z. Wenquan (✉) · P. Yaozhong
College of Resources Science and Technology,
Beijing Normal University,
Beijing 100875, People's Republic of China
e-mail: dyyucas@163.com

Introduction

Essentially, net primary productivity (NPP) is carbon fixed by the terrestrial ecosystem (Peng and Guo 2000). Solar radiation, temperature, precipitation, air humidity and carbon dioxide, which are the outside driving forces of the ecosystem, affect NPP by acting not only on vegetation directly, but also on the soil indirectly.

The changes of vegetation precipitation demand, temperature and atmospheric carbon dioxide concentration affect NPP most greatly. In a thousand-year interval, climate change is the main reason of vegetation change, and that non-climate factors are secondary (Whitlock and Bartlein 1997).The impact of climate change on NPP is realized by the interaction of temperature, precipitation and carbon dioxide, vegetation and soil (Chen et al. 1996; Willis et al. 1997; Epstein 1997). Precipitation affects NPP and its region distribution mainly by affecting water demand, water balance, carbon dioxide fixation of vegetation in the process of photosynthesis. Water deficit stress may result in leaf area attenuation (Kang et al. 1997), stoma close (Tang 1983) and transpiration and photosynthesis decline of the vegetation, so vegetation dry matter accumulation will drop. In general, properly increasing precipitation will prolong the growth period of vegetation, hence promoting NPP increase (Sala et al. 1988). Water as the stuff of vegetation photosynthesis plays an important role in the process directly, and on the other hand, it may affect NPP by adjusting temperature, vegetation water demand and nutriment elements supply (Melillo et al. 1993). In dry regions, precipitation is the master restricting factor to NPP, and NPP decreases with the ratio of precipitation and potential evaporation (Raich et al. 1991; Melillo et al. 1993). Precipitation and its season distribution are directly correlative with NPP in grassland, hungriness and wetland (Sala et al. 1988; Stephenson 1990). In some regions, there is a significant linear correlation between annually precipitation and above ground part of NPP (Sala et al. 1988). For the crop, the effect of the seasonal change of precipitation on its yield is greater (Whetton et al. 1993).

Atmospheric circulation system, which affects larger regions and lasts for a long time, may control the change of climate system in some regions by adjusting the distribution of precipitation and heat. In the northern hemisphere, researchers usually pay attention to some atmospheric circulation indices such as ENSO (El Nino/South Oscillation), Arctic Oscillation (AO), the North Atlantic Oscillation (NAO) pattern, the North Pacific (NP) index, the Pacific/North American (PNA)patterns, the Eurasian (EU) pattern, the West Atlantic (WA) pattern, the West Pacific (WP) pattern, East Atlantic (EA) pattern. NAO is the most notable mode in the northern Atlantic regions. Although it's most prominent scope is mainly in North America and Europe, climate system in some regions of Asia may feel its influence in spring (Dugam et al. 1997; Hurrell 1995). AO is the most important and largest area scale mode for the northern hemisphere during wintertime (Tompson et al. 2000) and is also notable until the coming spring (Tompson and Wallace 1998; Tompson et al. 2000).

Some researches have studied the responses of vegetation activity to climatic change (temperature and precipitation), and CO_2 increase (Goulden et al. 2000; Gong et al. 2002) and predicted climate change effects on vegetation, soil thermal dynamics and carbon cycling (Potter 2004), but detection of Large-scale Climate Signals in Spring NPP-precipitation coupling relationship is not reported until now. The first aim of this paper was to analyze the spatial response features of NPP in East Asia (70°E–170°E, 10°N–70°N) to spring precipitation, and the second task was to discuss the role of atmospheric circulation factors in the response.

Data

The remote sensing data used in this paper were NOVA/AVHRR (Earth Resources Observation System, Pathfinder AVHRR Land Data Set) NDVI (Normalized Difference Vegetation Index) sets for East Asia (70°E–1 70°E, 10°N–70°N) from 1982 to 1999, with 0.075×0.075° spatial resolution and monthly temporal resolution. The land cover data were downloaded from Maryland University (ftp://hpssftp.umiacs.umd.edu/project/GLCF/DerivedData/Global_Land_Cover/gl-latlong-8km-landcover). The climate data included monthly records of the precipitation, net radiation and average temperature, and all had the same image spatial resolution and projection type as the NDVI data set. Field measured NPP of different vegetation types came from the Oak Ridge National Laboratory Distributed Active Archive Center (NPP Database, http://www.daac.ornl.gov/NPP/npp_home.html) and National Forest Bureau of China. ENSO index came from Climate Prediction Center (USA). AO and NAO index were the observed value according to the definition by Tompson and Wallace (1998), and Hurrell (1995), respectively. NP index was the weighted mean air pressure of sea surface among 30–65°N and 160–140°W (Trenberth and Hurrell 1994). The definition of other five atmospheric circulation indexes can be found in Wallace and Gutzler's (1981) study.

Methodology

The model of estimating NPP

CASA (Carnegie–Ames–Stanford Approach) NPP model, whose calculation method can be found in the references (Field et al. 1995; Potter et al. 1993), is suitable to estimate NPP on a large geographical scale. Potter et al. (1993) and Filed et al. (1995, 1998) set the maximum light use efficiency to 0.389 gC·MJ^{-1} to drive CASA model and got 48.9 PgC (1 PgC=10^{15} g Carbon) for global NPP. Jeffrey (2006) used two data sets of NCEP (National Centers for Environment Prediction) and GISS (Goddard Institute for Space Studies) to drive CASA model so as to compare the quality of the two data sets, and he set the maximum light use efficiency of different vegetation types in the two data sets as 0.46 and 0.50 gC MJ^{-1}, respectively. Obviously, owing to the differences such as vegetation type, life type, the maximum light use efficiency for different vegetations should not be the same value. In this paper, we modeled the maximum light use efficiency for different vegetation types according to the principle of the minimum error between field NPP and estimated NPP. To some vegetation, the principle can be formulated as:

$$E(x) = \sum_{i}^{j} (m_i - n_i x)^2 \; x \in [l, u] \tag{1}$$

In formula 1, i and j express the sample number of the vegetation. m_i is field NPP and n is the product of APAR (absorbed photosynthetically active radiation), temperature and water deficit stress. x is the maximum light use efficiency modeled for the vegetation. l and u are the lower and upper light use efficiency of the vegetation,respectively. Formula 1 can be unwrapped as:

$$E(x) = \sum_{i}^{j} n_i^2 x^2 - 2\sum_{i=1}^{j} m_i n_i x + \sum_{i=1}^{j} m_i^2 \; x \in [l, u] \tag{2}$$

Formula 2 is a unary quadratic equation with an upward opening, so it has the minimum error from l to u. According to this principle, the maximum light use efficiency for different vegetation types in the study area are modeled as: Evergreen Needleleaf Forest 0.389 gC MJ^{-1}, Evergreen Broadleaf Forest 0.978 gC MJ^{-1}, Deciduous Needleleaf Forest 0.492 gC MJ^{-1}, Deciduous Broadleaf Forest 0.664 gC MJ^{-1}, Mixed Forest 0.490 gC MJ^{-1}, Woodland 0.572 gC MJ^{-1}, Wooded Grassland 0.557 gC MJ^{-1}, Closed Shrubland 0.541 gC MJ^{-1}, Open Shrubland 0.541 gC MJ^{-1}, Grassland 0.541 gC MJ^{-1}, Cropland 0.608 gC MJ^{-1}, Bare Ground and Urban and build-up 0.541 gC MJ^{-1}, Tundra 0.541 gC MJ^{-1}. It should be pointed that being short of filed NPP data for land covers of Bare Ground and Urban and build-up, the maximum light efficiency of the vegetation in these land covers was set to equal to that of Grassland. If there is no vegetation in Bare Ground type, namely the Normalized Different Vegetation Index (NDVI) equaling to 0, and NPP is also modeled as 0.

The method of analyzing the spatial response features of NPP to spring precipitation

We used the mathematical method of singular value decomposition (SVD), which can be found in the reference of Wallace et al. (1992), to study the coupling relationship between spring NPP and precipitation sequences. The paired-mode correlation coefficient was calculated by the corresponding temporal coefficient of the paired-mode between NPP and precipitation sequences. The region with higher correlation coefficient showed the close relationship between NPP and precipitation.

Linear regress model of the nine atmospheric circulation factors with NPP or precipitation

In some regions, NPP change may be impacted by multiple atmospheric circulation factors. At the same time, these factors may affect NPP pattern differently. It is necessary to differentiate the joint and individual impact on NPP of the nine atmospheric circulation factors.

To a pixel, there are normalized sequences Y_i (NPP) and Z_{1i}, Z_{2i}, ... Z_{ni}, which represent atmospheric circulation factors from 1 to n. The relationship of Y and Z can be formulated by multiple linear regression equation as:

$$\hat{Y} = b_1 Z_{1i} + b_2 Z_{2i} + \cdots b_n Z_{ni} \tag{3}$$

In Eq. 3, i is the time length (from 1982 to 1999 in this paper) and b_1, b_2,...and b_n are regression coefficients. There is the following relationship:

$$c^2 = b_1 r_1 + b_2 r_2 + \cdots b_n r_n \quad (4)$$

Where c^2 is multiple correlation coefficient and r_1, r_2,...and r_n are the correlation coefficients of NPP with the n atmospheric circulation factors (Z_{1i}, Z_{2i},... Z_{ni}), respectively. The left part of Eq. 4 is the joint impact of the n atmospheric circulation factors to NPP variance in the pixel and each item of the right part is the individual impact of Z_{1i}, Z_{2i},... Z_{ni}, respectively.

Results and discussion

The coupling features of spring NPP with precipitation

The results of SVD analysis showed that the response features of NPP to precipitation in spring were mainly embodied in the leading six NPP-precipitation paired-modes. The first to the sixth paired-mode could explain 42.91, 23.29, 9.96, 5.60, 5.04 and 3.95% covariance of NPP-precipitation, respectively (total to 90.75%). Temporal correlation coefficients of the leading six paired-modes were 0.830, 0.889, 0.841, 0.747, 0.912 and 0.923, respectively, and all the correlation was significant at the significant level of 0.001. So the relationship of spring NPP with precipitation was very close. Spatial features of the first and the second paired-mode were illustrated as Fig. 1a, b, and the figures for the other four paired-modes, which are relatively secondary, were omitted here. The first and the second paired-mode with relatively larger geographical scale were more important, which was generally the strongest NPP change center corresponding to the precipitation change center.

In the first paired-mode (Fig. 1a), the positive extreme value center of NPP was mainly located at the site in Thailand with latitude of 20°N and longitude of 100°E, corresponding to the positive value center of precipitation. The coupling negative extreme value center of NPP with precipitation was located at the site in Bengal with latitude of 25°N and longitude of 92°E. Change trend between NPP and precipitation near the areas of the two coupling center was synchronous. At the site with latitude of 57°N and longitude of 85°E in Guangdong province of China, change trend of positive NPP center and negative precipitation center was contrary.

In the second paired-mode (Fig. 1b), coupling NPP-precipitation center with negative extreme value in the latitude of 25°N and longitude of 93°E in Bengal showed the synchronous change trend between spring NPP and precipitation. In addition, in some areas of east China and parts of middle Japan, NPP and precipitation coupling centers with positive value also illustrated the synchronous change trend between spring NPP and precipitation.

In the whole, coupling features of NPP-precipitation in the areas of low latitude were more obvious than in the high latitude areas (Fig. 1). The main reason may be that temperature and heat conditions were the key restricting factors to vegetation growth in the high latitude areas in spring, but precipitation impacted vegetation growth more greatly in the low latitude areas.

Correlation analysis of NPP-precipitation paired-modes with atmospheric circulation factors

In this paper, we mainly considered the impact of the nine atmospheric circulation factors (AO, EA, EU, NAO, NP, PNA, SO, WA, WP) on NPP-precipitation coupling features. Correlation coefficients of NPP-precipitation paired-modes by singular value decomposition analysis with the nine atmospheric circulation factors were listed at Table 1.

There was no significant correlation in the first NPP-precipitation paired-mode, but the impact of AO, EU, NP and PNA was relatively important. The relationship of the second precipitation mode with NAO was closer, and correlation coefficient was 0.57. Correlation coefficients of the third precipitation mode with AO and SO were 0.47 and −0.55, respectively. Correlation coefficients of the fourth, fifth and sixth precipitation mode with WP, EA and EU were −0.47, 0.54 and 0.51, respectively. All the above correlation was significant at the significant level of 0.005. Correlation coefficients of the fourth and sixth NPP mode with WP and EU were −0.64 and 0.61, respectively, and the correlation was significant at the level of 0.001. Correlation coefficients of the fifth NPP mode with EU were 0.47, and the correlation was significant with the significant level of 0.005. So it could be concluded that AO, EA, EU, NAO, SO and WP

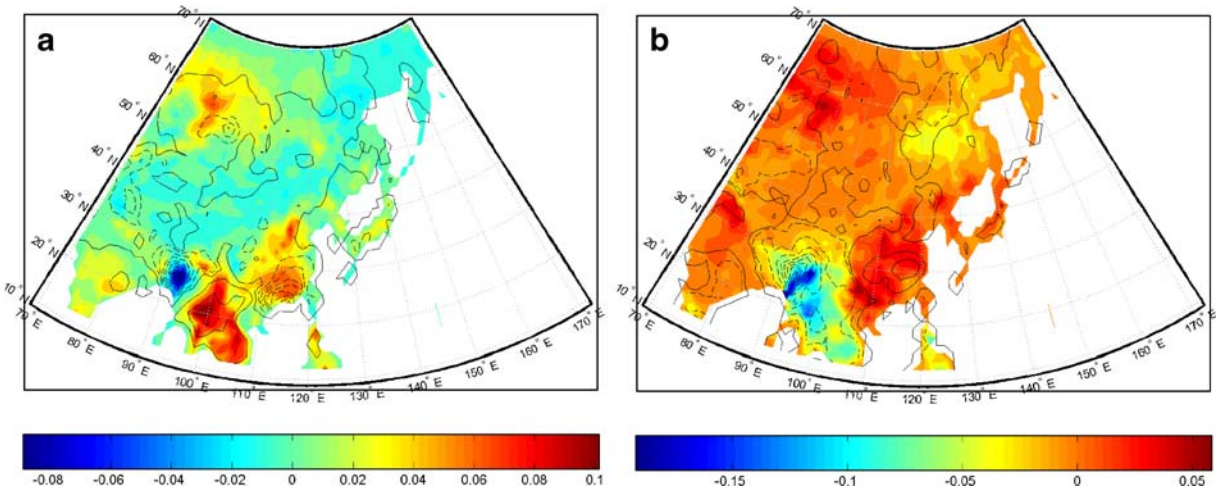

Fig. 1 The leading two paired-modes of spring NPP with precipitation by singular value decomposition analysis. NPP shown in *color*. Precipitation shown in *contours*, with an interval of 0.03. *Dashed lines* indicated the negative values and *solid lines* indicated the positive values. Zero contours were omitted for simplicity, and all the values are arbitrary and have no dimension. **a** and **b** are the first and the second paired-modes of spring NPP with precipitation, respectively, which indicate spatial coupling relationship between spring NPP and precipitation

impacted spring NPP and precipitation obviously. Especially, the impacts of EU on the sixth NPP-precipitation paired-mode, and WP on the fourth NPP-precipitation paired-mode was very great. When the signal of EU was strong, it was favorable to NPP and precipitation addition, but WP was contrary to this trend.

Individual atmospheric circulation factor had different impacts on different regions. Some regions may be impacted by many factors, and these factors usually tended to be dependent and jointly acted on climate system and vegetation. Table 2 showed the correlation of the nine atmospheric circulation factors with each other. There were significant correlations between NAO, NP, WA and AO, between NP and PNA, and between SO, WA, SO and PNA.

Regress analysis of NPP with atmospheric circulation factors

Observed NPP and the nine atmospheric circulation indexes were normalized firstly. To a pixel, regression equation could be built with NPP as the dependent

Table 1 Correlation coefficients of the temporal coefficient of NPP-precipitation paired-modes with the nine atmospheric circumfluence factors in spring

Paired-mode	AO	EA	EU	NAO	NP	PNA	SO	WA	WP
NPP 1	0.21	0.17	0.39	0.07	0.18	−0.26	0.04	−0.11	−0.08
Precipitation 1	0.22	−0.16	0.21	0.19	0.37	−0.46	0.24	−0.17	−0.15
NPP 2	0.13	0.01	0.08	0.47	0.07	−0.21	−0.31	0.07	−0.39
Precipitation 2	0.17	0.07	0.10	0.57[b]	−0.05	−0.15	−0.46	0.00	−0.40
NPP 3	0.34	0.27	0.02	0.11	−0.25	0.30	−0.46	−0.03	−0.23
Precipitation 3	0.47[b]	0.35	−0.03	0.23	−0.12	0.20	−0.55[b]	−0.13	−0.22
NPP 4	−0.37	−0.15	−0.18	−0.22	−0.25	0.18	−0.24	0.18	−0.64[a]
Precipitation 4	−0.46	−0.03	0.05	−0.35	−0.09	0.02	−0.08	0.17	−0.47[a]
NPP 5	0.21	0.45	0.47[b]	−0.05	0.27	−0.03	0.03	−0.13	0.39
Precipitation 5	0.03	0.54[b]	0.30	−0.26	0.13	0.10	−0.05	−0.07	0.28
NPP 6	−0.17	−0.08	0.61[a]	−0.15	0.11	−0.21	−0.14	−0.15	0.29
Precipitation 6	−0.16	−0.07	0.51[b]	−0.17	−0.03	−0.14	−0.29	−0.17	0.13

[a] The correlation was significant with significance level of 0.001

[b] The correlation was significant with significance level of 0.005

Table 2 Correlation coefficients of atmospheric circumfluence factors with each other in spring

Factors	AO	EA	EU	NAO	NP	PNA	SO	WA	WP
AO	1.00	−0.01	−0.11	0.77[a]	0.51[b]	−0.30	−0.01	−0.56[b]	0.15
EA		1.00	0.13	−0.24	−0.03	0.08	−0.39	0.16	−0.12
EU			1.00	−0.11	−0.05	0.07	−0.17	0.07	0.30
NAO				1.00	0.24	−0.16	−0.20	−0.34	0.01
NP					1.00	−0.83[a]	0.53[b]	−0.56[b]	0.14
PNA					a	1.00	−0.48[b]	0.43	0.14
SO							1.00	−0.06	0.37
WA								1.00	−0.17
WP									1.00

[a] The correlation was significant with significance level of 0.001

[b] The correlation was significant with significance level of 0.005

variable and the nine factors as the independent variables. According to the regression equation, calculated NPP value could be gotten. The ratio of calculated NPP variance with observed NPP variance reflected the joint impact of the nine factors on NPP change. The right part of formula 4 could differentiate the separate impact of the individual circulation factor on NPP change.

Interpretation rate of individual atmospheric circulation factor to NPP variance was listed in Table 3, and spatial distribution of the joint impact of the nine atmospheric circulation factors on NPP variance was illustrated as Fig. 2a. The areas with high interpretation rate of AO to NPP variance were mainly located in northeast China and Xinjiang municipality of China.

Table 3 Area percentage of the regions with NPP impacted by the individual atmospheric circulation factor (%)

Factors	Interpretation rate<30% (%)	30%< Interpretation rate <50% (%)	Interpretation rate>50% (%)
AO	87.60	8.22	4.18
EA	88.09	10.33	1.58
EU	84.81	11.31	3.88
NA	93.78	5.40	0.82
NP	96.14	3.36	0.50
PNA	93.16	4.93	1.91
SO	89.19	8.34	2.47
WA	86.55	12.84	0.61
WP	83.45	13.56	2.99

The area percentage in this table meant the ratio of the region with some interpretation rate to the whole region impacted by the atmospheric circulation factor. Interpretation rate means the proportion of NPP change during 1982–1999 caused by atmospheric circulation factor change.

The areas with high interpretation rate of EA to NPP variance were mainly located near latitude of 40°N such as Xinjiang municipality, Gansu province and Inner Mongolia of China, and some regions with latitude from 50°N to 66°N and longitude from 100°E to 140°E in Russia. The impact center of NP to NPP variance was centered in the regions within 50°N–70°N and 70°E–90°E. NAO mainly impacted the north part of Kamchatka Peninsula in Russia. The impact of NP on the study area was relatively weak in spring, and mainly focused within the scope of 20°N–40°N. PNA mainly affected north area of longitude 140°E, and SO mainly impacted NPP in the point with latitude of 57°N and longitude of 120°E. The high interpretation rate of WA to NPP variance was mainly located in the regions near the point with latitude of 50°N and longitude of 123°E, and WP mainly impacted the areas near the sea and with latitude scope from 20 N to 50°N and longitude scope from 110°E to 140°E.

The regions with the highest interpretation rate of the nine atmospheric circulation factors to spring NPP variance were mainly located within the latitude from 50°N to 65°N, especially the areas near the 60°N latitude line (see Fig. 2a). Percentages of the regions with interpretation rate over 80, between 50 and 80, and lower than 50% were 10.46, 55.12 and 34.42%, respectively. The percentage of the regions with interpretation rate over 50% totaled to 65.5 8%, so the nine atmospheric circulation factors impacted spring NPP greatly.

Vegetation growth process was controlled directly by many factors such as precipitation and temperature. Usually, atmospheric circulation system changes, and some local climate factors such as precipitation also

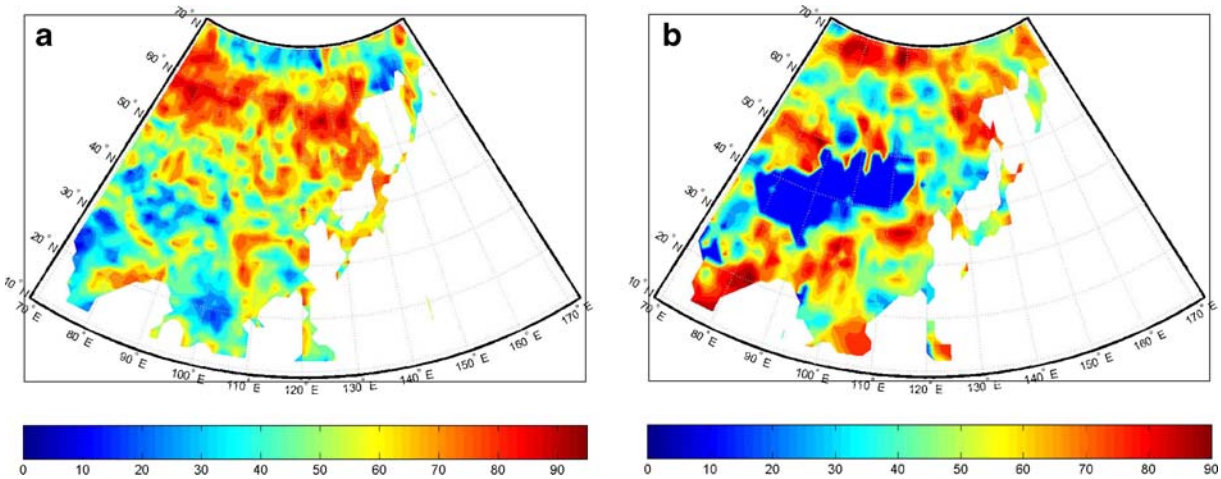

Fig. 2 The interpretation rates of atmospheric circumfluence factors to spring NPP variance (**a**) and spring precipitation variance (**b**)

changes subsequently. How does atmospheric circulation system affect the spatio-temporal pattern of precipitation? We also used the same regression method to choose precipitation of the pixel as the dependent variable and the nine atmospheric circulation factors as the independent variables, and built a multiple linear regression equation. Spatial interpretation rate of the nine atmospheric circulation factors to spring precipitation pattern was illustrated as Fig. 2b.

The percentages of the regions with interpretation rate over 80, between 50 and 80 and lower than 50% were 7.44, 52.9 and 39.66%, respectively. The nine atmospheric circulation factors explained 60.34% precipitation changes of the areas with interpretation rate to NPP-precipitation paired modes over 50%, so these factors impacted spring precipitation pattern greatly. Hungriness near the boundary of Northwestern China, Mongolia and Kazakstan (the dark blue areas in Fig. 2b) with little precipitation in spring was weakly influenced by the nine atmospheric circulation factors.

We chose three regions in Fig. 1a (Bengal (22–25°N, 90–93°E), south China (25–30°N, 110–115°E), and Thailand (16–25°N, 97–102°E) with distinct spatial NPP-precipitation coupling features to build multiple linear regression equation between NPP, precipitation and the nine atmospheric circulation factors, respectively. Correlation coefficients between observed NPP and calculated NPP for Bengal, south China and Thailand were 0.692, 0.748, and 0.762, respectively, and correlation coefficients between observed precipitation and calculated precipitation for Bengal, south China and Thailand were 0.712, 0.725, and 0.756, respectively. All the correlations were significant with significance level of 0.005, so the nine atmospheric circulation factors had a great effect on spatial NPP-precipitation coupling features in the three regions.

Interpretation rate of the nine atmospheric circulation factors to spring NPP was higher than spring precipitation in the latitude scope from 50°N to 65°N (Fig. 2). Coupling features of the leading paired-modes of NPP-precipitation in the latitude scope were not notable. Obviously, in the latitude scope from 50°N to 65°N, precipitation is one of the factors that affect spring NPP accumulation, but not the sole factor and there must have some factors such as temperature influencing spring NPP generation. Land surface above 50°N–65°N is widely covered with boreal coniferous forest, and a study has suggested that vegetation in these regions is sensitive to temperature change (Goulden et al. 1998). In the whole study area, the nine atmospheric circulation factors influenced coupling features of spring NPP and precipitation more greatly in the areas southern to latitude 30N°. Gong et al. (2002) and Kawabata et al. (2001) have also proved that spring vegetation activity in the northern hemisphere is sensitive to climate changes.

Although spring NPP and precipitation were impacted by the nine atmospheric circulation factors greatly in many regions, some change trends were still not explained completely. The regions with interpretation rater of the nine atmospheric circulation factors to spring NPP and precipitation lower than 50% still occupied great proportion. The possible reasons may be that: (1) local micro climate and other environment

conditions were not considered; (2) NPP change in the middle and high latitude areas may be more sensitive to temperature than to precipitation; (3) In some regions, the relationship of NPP and precipitation with the nine atmospheric circulation factors was not simply linear, so the multiple linear regression model is not suitable to study the relationship among them; (4) Besides the nine atmospheric circulation factors, other larger scale of climate system such as east Asian monsoon may greatly influence spring NPP and precipitation pattern. All these uncertain possibilities must be studied in the future work.

Conclusion

Spatial response features of spring NPP to precipitation are mainly included in the six leading paired-modes, which totally explain 90.75% of NPP-precipitation covariance. All correlations of the leading six temporal coefficients of NPP and precipitation are significant with the significant level of 0.001. So the relationship of spring NPP with precipitation is very close, and the most notable coupling features come out in the negative coupling core of Bengal (22–25°N, 90–93°E) and positive coupling core of Thailand (16–25°N, 97–102°E) in the first NPP-precipitation paired-mode by singular value decomposition.

Atmospheric circulation system plays an important role in coupling features of spring NPP with precipitation, and usually, they tend to work jointly. The percentages of the regions with interpretation rate of the nine atmospheric circulation factors to spring NPP and precipitation pattern over 50% total to 65.58 and 60.4 1%, respectively, so in many regions, spring NPP and precipitation are greatly influenced by these circulation factors.

Acknowledgments This paper was funded by the Program for New Century Excellent Talents in University of China. Thanks are due to referees and editors whose comments will improve the quality of the manuscript.

References

Chen, D. X., Hunt, H. W., & Morgan, J. A. (1996). Responses of a C_3 and C_4 perennial grass to CO_2 enrichment and climate change: Comparison between model predictions and experimental data. *Ecological Modeling*, *87*, 11–27.

Dugam, S. S., Kakade, S. B., & Verma, R. K. (1997). Interannual and long-term variability in the North Atlantic Oscillation and Indian Summer monsoon rainfall. *Theoretical and Applied Climatology*, *58*(1–2), 21–29.

Epstein, H. E., Lauenroth, W. K., & Burke, I. C. (1997). Productivity patterns of C3 and C4 functional types in the U S Great Plains. *Ecology*, *78*(3), 722–731.

Field, C. B., Behrenfeld, M. J., & Randerson, J. T. (1998). Primary production of the bio sphere: integrating terrestrial and oceanic components. *Science*, *281*, 237–240.

Field, C. B., Randerson, J. T., & Maimstrom, C. M. (1995). Global net primary production: combining ecology and remote sensing. *Remote Sensing of Environment*, *51*, 74–88.

Gong, D. Y., Shi, P. J., & He, X. Z. (2002). Spatial features of the coupling between spring NDVI and temperature over northern hemisphere. *Acta Geographica Sinica*, *57*(5), 505–514.

Goulden, M. L., Wofsy, S. C., Harden, J. W., Trumbore, S. E., Crill, P. M., Gower, S. T., et al. (1998). Sensitivity of boreal forest carbon balance to soil thaw. *Science*, *279*, 214–217.

Goulden, M. L., Wofsy, S. C., Harden, J. W., Trumbore, S. E., Crill, P. M., Gower, S. T., et al. (2000). Simulated responses of *Pinus halepensis* forest productivity to climatic change and CO_2 increase using a statistical model. *Global and Planetary Change*, *26*, 405–421.

Hurrell, J. W. (1995). Decadal trends in the North Atlantic Oscillation: regional temperatures and precipitation. *Science*, *269*, 676–679.

Jeffrey, A. H. (2006). NCEP and GISS solar radiation data sets available for ecosystem modeling: Description, differences, and impacts on net primary production. *Global Biogeochemical Cycles*, *19*, 1–18.

Kang, S. Z., Cai, H. J., & Liang, Y. L. (1997). On the study of the effects of elevated CO_2 concentration on the canopy temperature, evapotranspiration and soil water condition of spring wheat. *Acta Ecologica Sinica*, *17*(4), 412–417.

Kawabata, A., Ichii, K., & Yamaguchi, Y. (2001). Global monitoring of interannual changes in vegetation activities using NDVI and its relationship to temperature and precipitation. *International Journal of Remote Sensing*, *22*(7), 1377–1382.

Melillo, J. M., Kicklighter, D. W., & McGuire, A. D. (1993). Global climate change and terrestrial net primary production. *Nature*, *363*, 234–240.

Peng, S. L., & Guo, Z. H. (2000). Use of GIS and RS to estimate the light utilization efficiency of the vegetation in Guangdong, China. *Acta Ecologica Sinica*, *20*, 903–909.

Potter, C. (2004). Predicting climate change effects on vegetation, soil thermal dynamics, and carbon cycling in ecosystems of interior Alaska. *Ecological Modeling*, *175*, 1–24.

Potter, C. S., Randerson, J. T., & Field, C. B. (1993). Terrestrial ecosystem production: A process model based on global satellite and surface data. *Global Biogeochemical Cycles*, *7*, 811–841.

Raich, J. W., Rastetter, E. B., & Melillo, J. M. (1991). Potential net primary production in South America: application of a global model. *Ecological Applications*, *1*(4), 399–429.

Sala, O. E., Biondini, M. E., & Lauenoroth, W. K. (1988). Primary production of the central grasslands region of the United States. *Ecology*, *69*, 40–45.

Stephenson, N. L. (1990). Climatic control of vegetation distribution: The role of the water balance. *America Naturalist*, *135*(5), 649–670.

Tang, Z. C. (1983). On the study of drought ecophysiology in plants. *Acta Ecologica Sinia*, *3*(3), 196–203.

Tompson, D. W. J., & Wallace, J. M. (1998). The Arctic Oscillation signature in the wintertime geopotential height and temperature fields. *Geophysical Research Letters*, *25*, 1297–1300.

Tompson, D. W. J., Wallace, J. M., & Hegerl, G. C. (2000). Annular modes in the extratropical circulation, Part II: Trends. *Journal of Climate*, *13*, 1018–1036.

Trenberth, K. E., & Hurrell, J. W. (1994). Decadal atmospheric-ocean variations in the Pacific. *Climate Dynamics*, *9*, 303–319.

Wallace, J. M., & Gutzler, D. S. (1981). Teleconnections in the geopotential height field during the Northern Hemisphere winter. *Monthly Weather Review*, *109*, 784–812.

Wallace, J. M., Smith, C., & Bretherton, C. S. (1992). Singular value decomposition of Wintertime sea surface temperature and 500-mb height anomalies. *Journal of climate*, *5* (6), 561–576.

Whetton, P. H., Fowler, A. M., & Haylock, M. R. (1993). Implications of climate change due to enhanced greenhouse effect on floods and droughts in Australia and New Zealand. *Climatic Change*, *25*, 289–317.

Whitlock, C., & Bartlein, P. J. (1997). Vegetation and climate change in northwest America during the past 125 kyr. *Nature*, *388*, 57–60.

Willis, K. J., Braun, M., & Sumegi, P. (1997). Does soil change cause vegetation change or vice versa? A temporal perspective from Hungary. *Ecology*, *78*(3), 740–750.